A COMPANDING ALGORITHM AND SEGMENTATION OF HIGH DYNAMIC RANGE MAMMOGRAPHY IMAGES

Leka.K.K
PG Scholar
Department of ECE
Excel Engineering College
Komarapalayam - 600 025
Namakkal (Dist)
Tamil Nadu,India.
lekakumaran@gmail.com

Priyesh Kumar.A.T
Assistant Prfessor
Department of ECE
Excel Engineering College
Komarapalayam - 600 025
Namakkal (Dist)
Tamil Nadu,India.
atpkec@gmail.com

Kowtheesh.S
Assistant Prfessor
Department of ECE
Excel Engineering College
Komarapalayam - 600 025
Namakkal (Dist)
Tamil Nadu,India.
kowtheesh@gmail.com

Abstract- **The mammograms are high dynamic range (HDR) images having a 12 bit grayscale resolution. The screening mammography is currently the best procedure available for early detection of the breast cancer. When viewed by a radiologist, a single image must be examined several times, each time focusing on a different intensity range. Developed biologically derived mammography companding (BDMC) algorithm for compression, expansion, and enhancement of mammograms, in a fully automatic way. The BDMC is comprised of two main processing stages: 1) Preliminary processing operations which include standardization of the intensity range and expansion of the intensities which belong to the low intensity range. 2) Adaptively companding the HDR range by integrating multiscale contrast measures. The algorithm's performance has been preliminarily clinically tested on dozens of mammograms in collaboration with experienced radiologists. It appears that the suggested method succeeds in presenting all of the clinical information, including all the abnormalities, in a single low dynamic range companded image. This companded and enhanced image is not degraded more than the HDR image and can be analyzed without the need for professional workstation and its specific enhancement software. The segmentation process performed after completion of companding algorithm using level set implementation method. This segmented image identifies severity of cancerous tissues very easily.**

Index Terms—**Companding (compressing and expanding), high dynamic range (HDR), image enhancement, image segmentation, mammography.**

I. INTRODUCTION

Mammograms don't prevent breast cancer, but they can save lives by finding breast cancer as early as possible. For example, mammograms have been shown to lower the risk of dying from breast cancer by 35% in women over the age of 50. In women between ages 40 and 50, the risk reduction appears to be somewhat less. The acquired mammograms are high dynamic range (HDR) images having a 12–14 bit grayscale resolution.

The common display devices that have a low dynamic range (LDR) of 8 bit grayscale resolution cause the mammography images to have low contrast. Hence, we relate to studies that enhanced the mammograms through performance of contrast enhancement. Many reports on the contrast enhancement of mammography images relate to different algorithm families, such as several intensity windowing algorithms that have been developed. When using these types of algorithms, a small portion of the high intensity range of an image is selected and then remapped to a full intensity range of the display device

A. Work Flow

The schematic representation of the steps involved in BDMC algorithm is shown in Fig 3

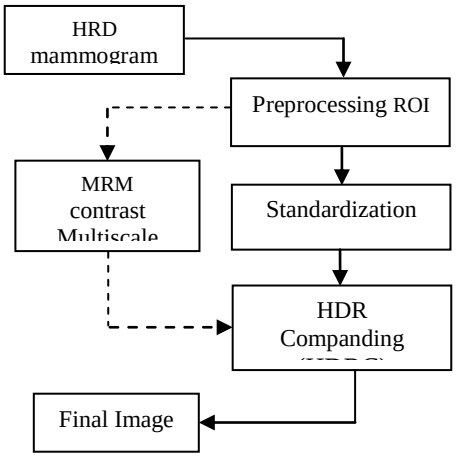

Fig 3 Work Flow of the Project

B. Biologically Derived Mammography Companding Algorithm

The suggested method has a specific mammography companding algorithm which is based on visual system models. It is termed biologically derived mammography companding (BDMC). The algorithm can be divided into two

main parts: preliminary stages which enable more efficient algorithm implementation and better visualization of the resultant image and the companding of the HDR mammography image.

1) Standardization and Low Intensity Expansion

Since the range of digital intensity values containing the breast tissue can vary significantly depending on the acquisition parameters, a standardization of the intensity range is required. The standardization is performed by equalizing gray levels of the cumulative distribution function (CDF) at 0.05 and 0.95 to specific values, chosen as representatives of the common intensity range. All the intensities of the input image are transformed using linear transformation which preserves the ratios between the intensity values. This standardization procedure forces the dark and bright areas of the image to be located at almost the same intensity range.

Since HDR algorithm works more effectively on high intensity levels of the image, preliminary contrast enhancement of low intensities is required. Thus, we expand the low contrast of the fatty tissues. An injective function (tone reproduction curve mapping) is implemented on the already standardized image. The mapping function consists of sigmoid function multiplied by power function

$$I_{exp}(x,y) = \frac{I_s(x,y)^b}{1+exp(-a(I_s(x,y)-c))} \quad (1)$$

whereas and *c* are constants that determine the slope and the position of the curve, respectively, and *b* determines the convexity of the curve. This specific mapping function enables expansion of low intensities while leaving the high intensities almost unchanged. For different adaptation levels, different response curves are obtained. In this example, the upper bold curve is a response curve before the adaptation. The arrow shows how the adaptation mechanism controls the gain of the system and yields the lower bold response curve.

2) High Dynamic Range Mammography Multiscale Companding:

The core of the algorithm is to compand (compress and expand) the HDR mammography image. The high dynamic range companding (HDRC) algorithm has been inspired by the adaptation mechanism of the visual system, i.e., the curve-shift mechanism. The HDRC algorithm will be explained in two main stages. The first stage describes the spatial building blocks (the retinal opponent receptive fields). This second stage describes the adaptation mechanism applied as a gain control mechanism. The adaptation mechanisms (local and remote) were performed separately for the center and the surround receptive field's sub regions. The adaptation of each sub region (center or surround) is influenced by the response of the remote region. Fig.3 presents a schematic structure of the HDRC algorithm.

a) Building Blocks of the Algorithm: The retinal ganglion receptive fields have spatial structure of "center" and "surround" masks. These opponent receptive fields have often been modeled in the literature by difference of Gaussians spatial mask. Additional annular shaped "remote" spatial maskf_r, has been added beyond the classical receptive fields of the "center",f_c and "surround"$f_s$masks. This remote area has not been added as a receptive field region, since it does not yield a response by itself, rather it modulates the response of the center and the surround regions.

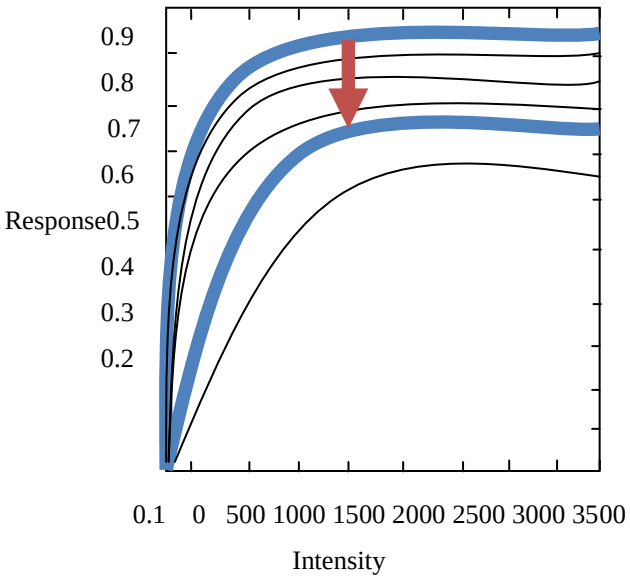

Fig 4Curve-shifting mechanism

The "center," "surround," and "remote" responses are calculated by convolving the output image of the previous stage,I_{exp} with the appropriate spatial masks$f_c f_s$, andf_r:

$$G_{cen}(i,j) = \sum_{center} \sum_{area} I_{exp}(x,y).f_c(i-x,j-y) \quad (2)$$

$$G_{cen}(i,j) = \sum_{surround} \sum_{area} I_{exp}(x,y).f_s(i-x,j-y) \quad (3)$$

$$G_{cen}(i,j) = \sum_{surround} \sum_{area} I_{exp}(x,y).f_s(i-x,j-y) \quad (4)$$

Since $f_c$has been applied with a size of one pixel, the G_{cen}response equals the imageI_{exp} .The flow chart for HDRC is shown in the Fig. 5 the algorithm has to be applied n varies parameters such as center, remote, and surround areas and the results are shown in the chapter 4 results and discussion.

b) Adaptation (Gain Control) Mechanism

The aim of adaptation is to increase the sensitivity of a system in a specific stimulus range in a specific physical domain. In the current adaptation mechanism of the retinal ganglion receptive fields, there is a transition from one response curve to another, resulting from a change in the light intensity of the local receptive field and its remote area, to obtain a higher gain in the new light intensity, Fig. 3.7. The "center" and the "surround" areas adapt separately, and only then the classical subtraction is done.

Hence

$$R = d_{cen}.\frac{G_{cen}}{G_{cen}+\sigma_{cen}} - d_{srnd}.\frac{G_{srnd}}{G_{srnd}+\sigma_{srnd}} \quad (5)$$

where d_{cen} and d_{srnd} are adaptation weight functions of each receptive field region. σ_{cen} Andσ_{srnd} are the adaptation functions that determine

$$\sigma_{cen} = \sigma_{cen},local + \sigma_{cen},remote \quad (6)$$

$$\sigma_{srnd} = \sigma_{srnd},local + \sigma_{srnd},remote \quad (7)$$

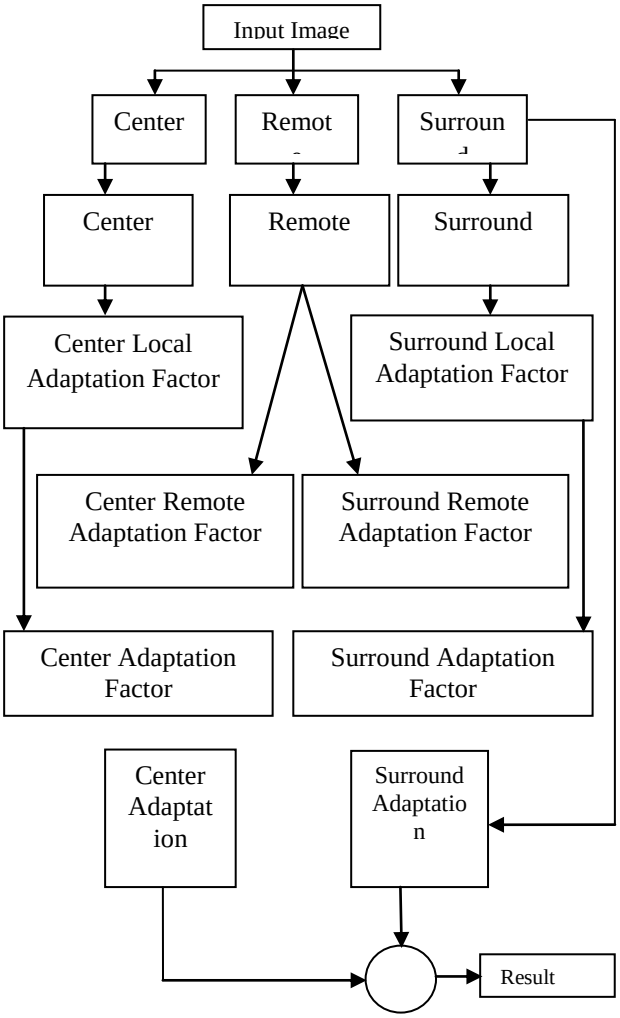

Fig 5 Flowchart of the HDRC algorithm.

The "local" components are

$$\sigma_{cen,local} = \alpha'_{cen} . G_{cen} + \beta_{cen} \quad (8)$$

$$\sigma_{srnd,local} = \alpha'_{srnd} . G_{srnd} + \beta_{srnd} \quad (9)$$

Where α is a parameter that determines the degree of the shifting the curve-shifting mechanism; β is a parameter that poses a "threshold" for the curve-shifting initiation. The degree of curve-shifting due to "local" and "remote" components.

The "remote" components are

$$\sigma_{cen,remote} = c_{cen} . MRM_{cen} . G_{remote} \quad (10)$$

$$\sigma_{srnd,remote} = G_{srnd} . MRM_{srnd} . G_{srnd} \quad (11)$$

where c is a parameter that determines the magnitude of the remote adaptation. The opponent receptive field total response

$$R = d_{cen} . \frac{G_{cen}}{\alpha'_{cen} . G_{cen} + \beta_{cen} + c_{cen} . MRM_{cen} . G_{remote}} - d_{srnd} . \frac{G_{srnd}}{\alpha'_{srnd} . G_{drnd} + \beta_{srnd} + c_{srnd} . MRM_{srnd} . G_{remote}} \quad (12)$$

(3.6)

Since the amount of expansion is determined due to local function which spreads over a large area (G_{remote}), the response$R$, is a non-injective operation. This property is expressed in the "thickness" of the response curve, which reflects the amount of adaptation, Fig. 6.

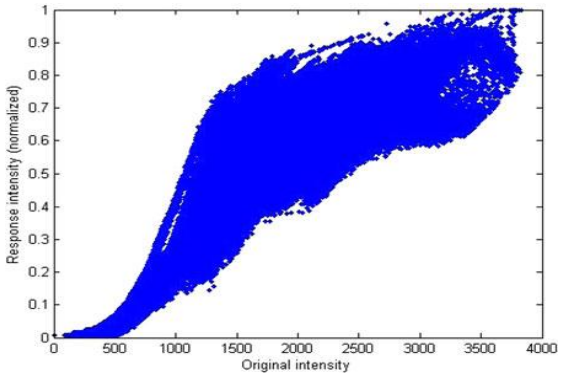

Fig. 6 Example of a response curve after the adaptation took place.

c) Multiscale Remote Modulation (MRM) Function: We aimed to determine the amount of expansion that the curve-shifting mechanism causes through the amount of local contrast. Since mammographic images have no clear edges (the glandular tissue looks like a "pack of clouds"), we had to apply new measures for texture contrast, in accordance with the requirements for mammography images. (This texture contrast has been motivated by computations that have been done on components of model for adaptation of the second order, at post retinal receptive fields). The modulations MRM_{cen} and MRM_{srnd} to the adaptation functions σ_{cen} and σ_{srnd} , respectively, are determined by approximation of the relative local texture contrast in relation to the maximum texture contrast in the image.

$$MRM_{cen} = C_{local,max} - C_{local} \quad (13)$$

$$MRM_{srnd} = C_{remote,max} - C_{remote} \quad (14)$$

Where C_{local} and C_{remote} are the multiscale local and remotecontrast quantifiers (in order to identify the specific texture edgesin the mammogram) of the initially preprocessed input image *I*.

The $C_{local,max}$ and $C_{remote,max}$ are the maximum contrast values of each contrast quantifier. The suggested method includes DOG filters of several resolutions that have the "center– surround" structure.

The "center" signal is defined as a convolution between the input image *I*, and a Gaussian decaying spatial weight function, f_c^k:

$$L_{cen}^k(i,j) = \sum_{center} \sum_{area} I(x,y) . f_c^k(i-x, j-y) \quad (15)$$

where k represents the specific spatial resolution. The larger the k value the coarser the spatial resolution (k = 1 is the finest resolution). fc is defined as

$$\rho_{remote}^{k} = \frac{1}{\pi.\rho_{cen}^{k\ 2}}.\exp(-\frac{x^2+y^2}{\rho_{cen}^{k\ 2}}) \quad (16)$$

Where ρ_{cen} represents the radius of the center region of thereceptive field. The "surround" signal is similarly defined

$$L_{srnd}^{k}(i,j) = \sum_{suuround} \sum_{area} I(x,y).f_c^k(i-x,j-y) \quad (17)$$

and $f_s$is a decaying Gaussian over the surround area

$$f_s^k(x,y) = \frac{1}{\pi.\rho_{srnd}^{k\ 2}}.\exp(-\frac{x^2+y^2}{\rho_{srnd}^{k\ 2}}) \quad (18)$$

Where ρ_{srnd}^{k} represents the radius of the surround area of thereceptive field. At each resolution, the surround mask has threetimes larger support area and a radius two times larger than thatof the center mask

$$\rho_{srnd}^{k} = 2.\rho_{cen}^{k} \quad (19)$$

The weight functions of $f_c$and$f_s$is normalized to 1. The total response at each resolution is calculated as a subtraction of the center and the surround responses of the appropriate resolution

$$L_{local}^{k} = L_{cen}^{k} - L_{srnd}^{k} \quad (20)$$

The local contrast quantifier is computed as a Gaussian weighting of the sum of the values of all resolutions:

$$C_{local}(i,j) = \sum_{local} \sum_{area} \left(\sum_{k-1} L_{local}^{k}\right)(x,y).W_{local}(i-x,j-y) \quad (21)$$

The kernel W_{local} is a Gaussian decaying spatial weightfunction

$$W_{local}(x,y) = \frac{1}{\pi.\rho_{local}^{k\ 2}}.\exp(-\frac{x^2+y^2}{\rho_{local}^{k}}) \quad (22)$$

whereρ_{local} is the radius of the local region. The remote contrast quantifier is computed with an additional Gaussian decaying kernel with an annular shape.

$$C_{remote}(i,j) = \sum_{remote} \sum_{area} C_{local}(x,y).W_{remote}(i-x,j-y) \quad (23)$$

$$W_{remote}(x,y) = \frac{1}{\pi.\rho_{remote}^{2}}.\exp(-\frac{x^2+y^2}{\rho_{remote}^{k}}) \quad (24)$$

Where ρ_{remote} is a radius of the remote area. Both Gaussianweighting kernels are normalized to 1.

3 Mapping Functions and Mask Properties

a) Standardization and Low Intensity Expansion: The mapping function parameters are the following: a =0.011, b = 0.8 and c is calculated adaptively as the average intensity of pixels that are considered to be within the fatty tissue.

b) High Dynamic Range Mammography

Multiscale Companding: Each pixel of the input image was simulated as the center region of the opponent receptive field. Accordingly, the "center"$f_c$mask has a radius of 1 pixel. The intensity range surround region of the "surround" $f_s$mask was defined as having an outer radius of13 pixels excluding the central pixel. The "remote" mask $f_r$hasan annular shape with inner and outer radii of 13 and 39 pixels, respectively. The inner radius of the "remote" is equal to the external radius of the "surround" and therefore does not overlap the "center" or the "surround" regions. The

Table 1 Masks Properties [pixels]

Resolution index	f_{cen}^{k}	ρ_{cen}^{k}	f_{srnd}^{k}	ρ_{srnd}^{k}
1	1	1	3	2
2	3	3	9	6
3	5	5	15	10
4	7	7	21	14
5	9	9	27	18
6	11	11	33	22

spatial functionsf_c,f_s and $f_r$are represented by Gaussian decaying profiles with appropriate variances. The total weights of these functions are normalized to 1. All of the masks' properties are summarized in Table 1.

The Spatial structure of "local" and "remote" areas and multiscale center surround". The circles of different sizes illustrate the "center-surround" masks of different resolutions. The inner circle area illustrates the "local" area that is defined by a Gaussian kernelW_{local}. The outer ring illustrates the "remote" area that is defined by an annulus like Gaussian kernelW_{remote}.

The adaptation function parameter values are summarized in Table 2. These values are the optimal values we have selected over a large number of simulations on a vast variety of mammograms. The chosen values were used across all of the processed mammograms. The values of mask patterns and the HRDC algorithm parameters to be applied to the HRDC algorithm then the resulting enhancement are obtained. The major practical contribution of this study in companding the HDR mammography images to LDR mammography images might lie in the important benefits of using the algorithm clinical settings. The algorithm succeeds to compress and expose all of the details from the original images.

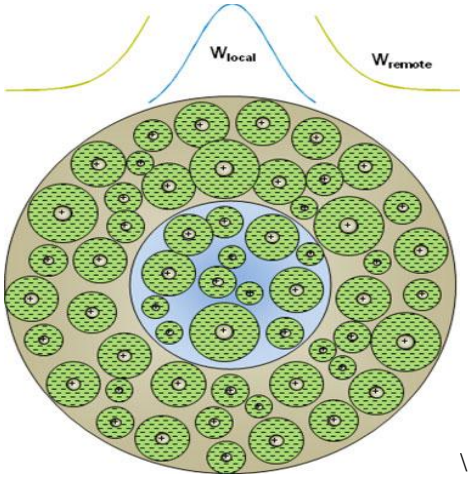

Fig 7 Spatial structure of "local" and "remote" areas and multiscale center surround "filters for contrast quantifier computations.

Table 2 HDRC algorithm parameters

Parameter	Value	Parameter	value
α_{cen}	1	α_{srnd}	1
β_{cen}	2	β_{srnd}	2.5
C_{cen}	1.4	C_{srnd}	2
d_{cen}	1	d_{srnd}	0.2

c) Multiscale Remote Modulation (MRM) Function: Local multiscale contrast is calculated over six resolutions. The mask sizes and their radii differ between each two subsequent resolutions by 2 pixels. For each resolution the center radius is the same size as the mask size. The radius for the matching surround mask is twice as large. The full details of the different mask sizes and their compatible radii, both of "center" f_c^k and "surround" f_s^k regions, at different resolutions, are summarized in Table 3.The calculations of the C_{local} quantifier were performed witha ρ_{local} radius (variance of Gaussian profile) of 4 pixels. The calculations of the C_{remote} quantifier were performed with a Fig. 7.

Table 3 MRM masks properties

Mask type	Inner Radius	External Radius	Variance
f_c	-	1	-
f_s	1	13	14
f_r	13	39	40

d) Visual Validation

The Fig 8 (a) shows benign images often contain abnormalities, but without clinically relevant findings, which presents lower and upper seromas (cavities filled with fluids due to lumpectomy). The final result Fig 4.1 (b) shows significant contrast improvement of all the intensity zones.

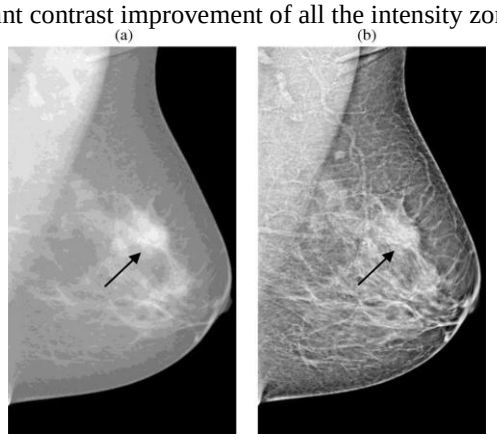

Fig 8 The arrow points to a carcinoma with a speculated mass shape. (a) Original image. (b) BDMC algorithm result.

II. CONCLUSION

BDMC algorithm performs companding through a "curve-shifting" mechanism, while determining the amount of compression based on a specific multiscale contrast measure that has been suggested originally for the visual system. The algorithm succeeds to compress and expose all of the details (including diagnostic information) from the original image, which is an HDR image, to an LDR image. This algorithm has the potential to enable the physicians to observe the mammograms without the need for professional workstations and it specific enhancement software.

III. FUTURE WORK

The future enhancement will be segmentation of cancerous cells from this enhanced mammography images. The level set method of segmentation is very adaptive for this type of segmentation. This method will be used for segmentation of features. It is very useful for identifying of the severity of the carcinoma and cancerous cells easily.

REFERENCES

[1] H. D. Cheng and H. Xu, (2002) "A novel fuzzy logic approach to mammogram contrastenhancement," Inf. Sci., vol. 148, pp. 167–184.

[2] J. Jiang, B.Yao, andA. M.Wason,"Integration (2005)of fuzzy logic and structure tensor towards mammogram contrast enhancement"Comput. Med.Imag.Graph.vol.29, pp. 83–90.

[3] J. K. Kim, J. M. Park, K. S. Song, and H. W. Park, (1997) "Adaptive mammographic image enhancement using

first derivative and local statistics," IEEE Trans. Med. Image. vol. 16, pp. 495–502.
[4] A. F. Laine, S. Schuler, J. Fan, and W. Huda, (1994) "Mammographic feature enhancement by multiscale analysis," IEEE Trans. Med. Imag., vol. 13, no. 4, pp. 725–739.
[5] A. F. Laine, J. Fan, and S. Schuler, (1994) "A framework for contrast enhancement by dyadic wavelet analysis," in Proc. 2nd Int. Workshop DigitalMammography, pp. 91–100.
[6] A. F. Laine, S. Song, J. Fan, W. Huda, J. C. Honeyman, and B. C. Steinbach, (1993) "Adaptive multiscale processing for contrast enhancement," in Proc. SPIE, pp. 521–532.
[7] Leon Kanelovitch, Yaakov Itzchak, ArieRundstein, MiriSklair, and Hedva Spitzer, (1995) "Wavelets for contrast enhancement of digital mammography," IEEE Eng. Med. Biol. Mag., vol. 14, no. 5, pp. 536 550.
[8] Leon Kanelovitch, Yaakov Itzchak, ArieRundstein, MiriSklair, and Hedva Spitzer (2013) "Biologically Derived Companding Algorithm for High Dynamic Range Mammography Images" vol. 60, no. 8.
[9] S. M. Pizer, E. P. Amburn, J. D. Austin, R. Cromartie, A. Geselowitz, T.Greer, B. H. Romeny, J. B. Zimmerman, and K. Zuiderveld, (1987)"Adaptive histogram equalization and its variations," Computer Vision, Graphics, Image Process, vol. 39, pp. 355–368.
[10] E. D. Pisano, E. B. Cole, B. M. Hemminger, M. J. Yaffe, S. R. Aylward, A. D. A. Maidment, R. E. Johnston, M. B. Williams, L. T. Niklason, E. F. Conant, L. L. Fajardo, D. B. Kopans, M. E. Brown, and S. M. Pizer, (2000) "Image processing algorithms for digital mammography: Apictorial essay," Radio graphics, vol. 20, pp. 1479–1491.
[11] A. M. Reza, (2004) "Realization of the contrast limited adaptive histogram equalization (CLAHE) for real-time image enhancement," J. VLSI Signal Process., vol. 38, pp. 35–44.
[12] F. Sahba and A. Venetsanopoulos, (2008) "Contrast enhancement of mammography images using a fuzzy approach," in Proc. 30th Ann.Int. Conf. IEEEEng. Med. Biol. Soiety, pp. 2201–2204.
[13] P. Sakellaropoulos, L. Costaridou, and G. Panayiotakis, (2003) "A wavelet- based spatially adaptive method for mammographic contrast enhancement," Phys. Med. Biol., vol. 48, pp. 787–803.
[14] F. Sahba and A. Venetsanopoulos,(2008) "Contrast enhancement of mammography images using a fuzzy approach," in Proc. 30th Ann.Int. Conf. IEEEEng. Med. Biol. Soiety, pp. 2201–2204.

